Simulation of dielectric resonator for a high-T_c radio frequency superconducting quantum interference device*

Gao Ji(高 吉), Yang Tao(杨 涛), Ma Ping(马 平)†, and Dai Yuan-Dong(戴远东)

School of Physics and State Key Laboratory for Artificial Microstructure and Mesoscopic Physics, Peking University, Beijing 100871, *China*

(Received 10 November 2009; revised manuscript received 4 December 2009)

Nowadays, the high-critical-temperature radio frequency superconducting quantum interference device (high-T_c rf SQUID) is usually coupled to a dielectric resonator that is a standard $10 \times 10 \times 1$ mm^3 $SrTiO_3$ (STO) substrate with a $YBa_2Cu_3O_{7-\delta}$ (YBCO) thin-film flux focuser deposited on it. Recently, we have simulated a dielectric resonator for the high-T_c rf SQUID by using the ANSOFT High Frequency Structure Simulator (ANSOFT HFSS). We simulate the resonant frequency and the quality factor of our dielectric resonator when it is unloaded or matches a 50-Ω impedance. The simulation results are quite close to the practical measurements. Our study shows that ANSOFT HFSS is quite suitable for simulating the dielectric resonator used for the high-T_c rf SQUID. Therefore, we think the ANSOFT HFSS can be very helpful for investigating the characteristics of dielectric resonators for high-T_c rf SQUIDs.

Keywords: dielectric resonator, YBCO, rf SQUID, HFSS

PACC: 7490, 7790

1. Introduction

The radio frequency superconducting quantum interference device (rf SQUID) consists of a single Josephson junction that interrupts a superconducting loop. The loop is inductively coupled to a tank circuit (i.e. a resonator) that is driven by an rf signal oscillating near the resonant frequency.

Since the discovery of high-critical-temperature (high-T_c) superconductivity in 1986,[1] the study of high-T_c rf SQUIDs operating at the boiling point of liquid nitrogen (∼77 K) has made great progress. Despite the wide variety of high-T_c superconducting cuprates, so far almost all high-T_c rf SQUIDs are made of $YBa_2Cu_3O_{7-\delta}$ (YBCO). This is largely because only the YBCO film with its *c*-axis normal to the substrate ("*c*-axis YBCO film") has been shown to have the sufficiently strong flux pinning at 77 K to ensure both the high critical current density in the *ab* plane and the acceptably low level of $1/f$ noise.[2] Although the early thin-film YBCO rf SQUIDs[3,4] were coupled to traditional lumped element LC tank circuits and operated at bias frequencies of 20–30 MHz or 150–160 MHz, the later ones[5−11] were coupled to various kinds of resonators biased at frequencies in a microwave range, and they achieved lower levels of flux noise because of their higher bias frequencies. Besides relatively high bias frequency, the optimization of the high-T_c rf SQUID also needs a high loaded quality factor of the resonator. Eventually, three relatively mature and simple high-T_c rf SQUID types were established. They all employed a washer-shaped thin-film YBCO rf SQUID, but the resonators used for them were a superconducting coplanar resonator, a superconducting thin-film comb resonator, and a dielectric $SrTiO_3$ (STO) substrate resonator with a flux concentrator deposited on it, respectively.

The superconducting coplanar resonator consists of two concentric stripes surrounding a flux-focusing large washer, both patterned from the same YBCO thin film; the superconducting thin-film comb resonator consists of an open YBCO thin-film loop whose two ends are comb-shaped. These two types of YBCO resonators are both usually deposited on $LaAlO_3$ (LAO) crystal substrates. Their unloaded quality factors at 77 K are typically a few thousand and their loaded quality factors, when they are coupled to the SQUID and the electronics, are typically in a 200–300 range. While coupled to the superconducting coplanar

*Project supported by the National Basic Research Program of China (Grant No. 2006CB601007), the National Natural Science Foundation of China (Grant No. 10674006), the National High Technology Research and Development Program of China (Grant No. 2007AA03Z238), and the Foundation of the State Key Laboratory of Information Control Technology for Communication System, China (Grant No. 9140C1304010803).

†Corresponding author. E-mail: maping@pku.edu.cn

© 2010 Chinese Physical Society and IOP Publishing Ltd

resonator or the superconducting thin-film comb resonator, the washer-shaped YBCO rf SQUID may show quite a low white flux noise of about $1\times10^{-5}\Phi_0/\mathrm{Hz}^{1/2}$ at frequencies above 100 Hz but rather a high low-frequency flux noise of not less than $5\times10^{-5}\Phi_0/\mathrm{Hz}^{1/2}$ at 1 Hz. In order to reduce the low-frequency flux noise of the washer-shaped YBCO rf SQUID, now people often replace the coplanar resonator or the comb resonator by the dielectric $SrTiO_3$ (STO) substrate resonator. Because the very large dielectric constant of the STO material can lead to a confinement of the resonator rf field within the STO substrate, the influence of the environment on the rf field distribution of the washer-shaped YBCO rf SQUID coupled to the dielectric resonator may be reduced, and thus the influence of the environment on the operating point of the rf SQUID may also be reduced, which may bring on an obvious reduction of the flux noise in the low-frequency range.[8]

The dielectric resonator used for the high-T_c rf SQUID is a standard $10\times10\times1$ mm^3 STO substrate with a YBCO thin-film flux focuser deposited on it. He *et al.*[12] once simulated a dielectric resonator for the high-T_c rf SQUID by using SONNET SUITES high frequency electromagnetic (EM) software. They simulated the resonant frequency and the quality factor of the dielectric resonator with or without the SQUID coupled to it, and the simulated values were in good agreement with the practical measurements. Recently, we simulated a dielectric resonator for the high-T_c rf SQUID, too. Instead of using SONNET EM software, we used ANSOFT High Frequency Structure Simulator (ANSOFT HFSS) to simulate the resonant frequency and the quality factor of the dielectric resonator, and our simulation results are also quite close to the practical measurements.

2. Simulation of frequency and quality factor of our dielectric resonator

ANSOFT HFSS is a high-performance full-wave electromagnetic field simulator for three-dimensional (3D) volumetric passive device modeling. In this software the finite element method (FEM) and the adaptive meshing are adopted. The basic mesh element of HFSS is a tetrahedron, thus this software is suitable for solving any arbitrary 3D geometry.

The HFSS has three available solution types: driven modal, driven terminal, and eigenmode. In this paper, we set the solution type to be eigenmode type when we calculate the eigenvalues of the resonant frequency and the quality factor of our dielectric resonator, and set the solution type to be driven terminal type when we calculate the resonant frequency and the quality factor of our dielectric resonator coupled to a transmitter–receiver coil and a 50-Ω coaxial cable, both of which are necessary parts of our experimental setup for measuring the dielectric resonator resonance.

2.1. Eigenvalues of resonant frequency and quality factor of our dielectric resonator

A $10\times10\times1$ mm^3 (100) STO substrate was used to fabricate the dielectric resonator. We deposited a YBCO thin film with a thickness of about 100 nm on the substrate, and then patterned the film by ultraviolet lithography to obtain a washer flux concentrator. The outer dimensions of the flux concentrator were 10×10 mm^2, which were the same as the substrate area; the inner hole of the flux concentrator had a diameter of 1 mm, and the slit of the flux concentrator had a width of 0.5 mm.

To investigate the resonance characteristic of our dielectric resonator, we first calculated the eigenvalues of the resonant frequency and the quality factor of it, using the eigenmode solver of HFSS.

The parametric model in the simulation was composed of the dielectric resonator that was in the middle of a column of liquid nitrogen. Outside the column of liquid nitrogen, there was the vacuum background automatically assigned by the HFSS. In our model, the STO substrate and the column of liquid nitrogen were all solid objects. The outer boundary of the STO substrate was a box with dimensions of $10\times10\times1$ mm^3. Because the HFSS can automatically define any object surface that touches the background as a perfect electric (perfect E) boundary, all the outer surfaces of the column of liquid nitrogen should be far enough from the STO substrate to ensure that they have no significant effect on the resonance characteristic of the dielectric resonator. In fact, we let the lateral surface of the column of liquid nitrogen have a diameter of 100 mm; set the distance between the top and the bottom surfaces of the column of liquid nitrogen to be 51 mm, so that each of them was 25 mm far from the

counterpart surface of the STO substrate. In order to save memory in the simulating process, we set the YBCO flux concentrator to be a sheet with a thickness of zero. But its values of outer dimension, inner hole diameter and slit width were the same as the real YBCO's. Ignoring the surface resistance and kinetic inductance of the real YBCO thin film at 77 K, we assigned a perfect E boundary to the YBCO flux concentrator in our model. To our knowledge, the dielectric constants of liquid nitrogen and STO at 77 K are about 1.4 and 2000, respectively; the dielectric loss of the STO crystal we used is about 3×10^{-4} at 77 K. Thus, we adopted these data in our model.

Using the eigenmode solver, we calculated the first resonant mode of our model with the frequency not less than 300 MHz. In order to obtain pretty accurate simulation results, we let the maximum refinement per pass be quite a high value, 20%, so that the tetrahedral mesh increased approximately 20 percent for each adaptive pass. Besides this, we set the maximum delta frequency per pass to be 0.01%, and set the minimum number of converged passes to be 2, which meant that if the delta frequency (i.e. the percentage difference between calculated eigenmode frequencies from one adaptive pass to the next) was more than 0.01%, the adaptive analysis would continue, and that the adaptive analysis would not stop until there had been two consecutive passes each having a delta frequency not more than the small upper limit 0.01%. Because the above convergence criterion was strict enough and might be achieved through many adaptive passes, we set the maximum number of passes to be as high as 30. In fact, after completing 12 passes, the solver gave the final results: a frequency of 464.397 MHz, and a quality factor of 3342.58. Those are the calculated eigenvalues of resonant frequency and quality factor of our resonator.

2.2. Resonance of our dielectric resonator matching 50-Ω impedance

The practical setup for measuring the resonance characteristics of our dielectric resonator was a one-port system, in which a copper coil was used as a transmitter–receiver coil and a 50-Ω coaxial cable connected the coil to the readout electronics. In our practical measurement, we must measure the resonance curve of our resonator matching the 50-Ω impedance of the coaxial cable. The 50-Ω matching could be realized by adjusting the distance between the copper coil and the resonator.

To simulate the resonance curve in our practical measurement, we employed the driven terminal solver of HFSS. This time the parametric model was composed of the dielectric resonator, the copper coil, a column of liquid nitrogen surrounding them, and a wave port with an impedance of 50-Ω. In this model, the dielectric resonator was the same as the one we mentioned in Subsection 2.1. Above the YBCO flux concentrator, there was the copper coil, which was concentric with the flux concentrator and had an outer diameter of 7 mm and a line width of 1-mm. The resonator and the coil were surrounded by the column of liquid nitrogen, which was very similar to the one we mentioned in Subsection 2.1 but had an upper surface that was assigned to be a radiation boundary and was connected to two 1-mm long leads of the copper coil. The ends of the two leads of the copper coil were in the middle of the wave port, which was a small rectangle plane overlapping the upper surface of liquid nitrogen. The wave port allowed the excitation signal to enter and leave the copper coil through it. The wave port contained a terminal, which touched one coil lead while the other coil lead was regarded as a reference conductor.

At first, we set the distance h between the copper coil and the resonator to be 4 mm. We chose 464 MHz as the solution frequency (i.e. the frequency at which the adaptive analysis was performed), let the maximum refinement per pass be 20%, set the maximum delta S per pass to be 0.02, assigned the minimum number of converged passes to be 2, and let the maximum number of passes be as high as 30. And, we added a fast frequency sweep in our solution, whose frequency ranged from 459 MHz to 469 MHz. In order to ensure the solution accuracy, we assigned 0.002 MHz to be the step size for the fast sweep. After successfully performing the adaptive analysis at 464 MHz and the fast frequency sweep based on it, the solver gave the relation curve of S-parameter versus frequency (i.e. the simulated resonance curve), which is a resonance hump whose apex is at a frequency of 465.866 MHz (see Fig. 1). However, because the solution frequency 464 MHz is not within the 3-dB frequency band, this curve may be not very credible. Therefore, we assigned 465.7 MHz to be the solution frequency, set the fast sweep frequency range to be 460.7–470.7 MHz, and let the solver perform the adaptive analysis and fast sweep again. This time we obtained a resonance curve whose resonant frequency f_0 was 466.010 MHz, resonance amplitude

was about 27.5 dB and 3-dB frequency band was from 465.686 MHz ($f_{\rm L}$) to 466.332 MHz ($f_{\rm H}$), so the solution frequency 465.7 MHz is within the 3-dB frequency band (see Fig. 2). Using the simulated resonant frequency and 3-dB frequency band, we easily calculated the loaded quality factor Q to be

$$Q = \frac{f_0}{\Delta f} = \frac{f_0}{f_{\rm H} - f_{\rm L}} = \frac{466.010\ \text{MHz}}{466.332\ \text{MHz} - 465.686\ \text{MHz}} = 721. \quad (1)$$

In the above expression, $f_{\rm L}$ and $f_{\rm H}$ are the start and the stop frequencies of the 3-dB frequency band, respectively; $\Delta f = f_{\rm H} - f_{\rm L}$ is the width of the 3-dB frequency band.

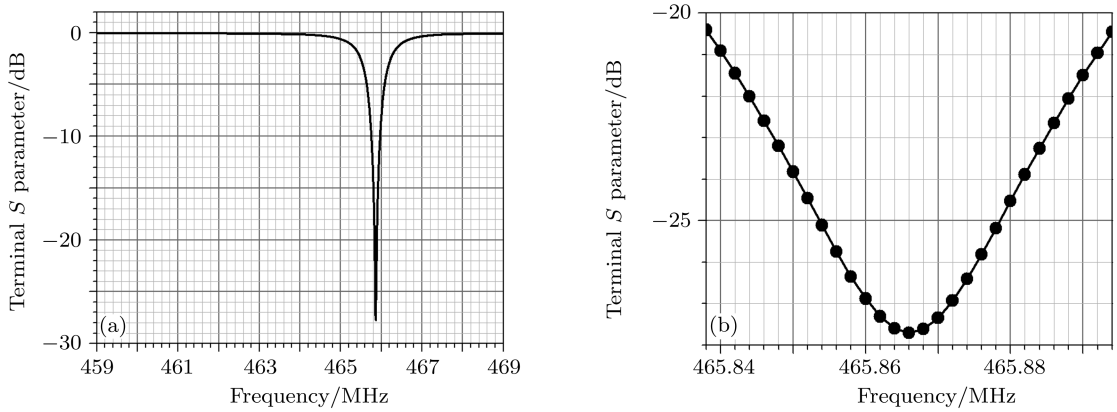


Fig. 1. Simulated resonance curve of our resonator (for h = 4 mm, solution frequency = 464 MHz), showing the whole resonance curve (a) and the details of the resonance curve apex (b) where the solid circles represent the simulation data.

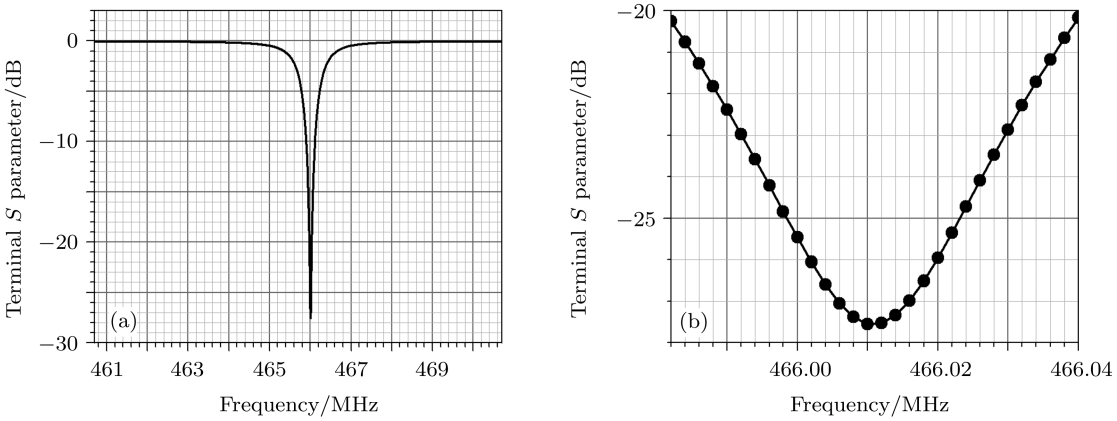


Fig. 2. Simulated resonance curve of our resonator (for h = 4 mm, solution frequency = 465.7 MHz), showing the whole resonance curve (a) and the details of the resonance curve apex (b) where the solid circles represent the simulation data.

In practical measurement, we may consider that our resonator is a nice match for the transmitter–receiver coil and 50-Ω coaxial cable if we obtain a resonance curve with a resonance amplitude not less than 20 dB, and, as a rule of thumb, the resonance amplitude may be influenced by the distance between the transmitter–receiver coil and the resonator. Therefore, it is not sufficient to simulate only one resonance curve corresponding to a certain distance h between the copper coil and the resonator when we research the resonance characteristics of our resonator matching the 50-Ω impedance, and we should simulate resonance curves corresponding to different values of h as many times as possible, as long as their resonance amplitudes are not less than 20 dB.

In fact, besides h = 4 mm, we also simulated the resonance curves for h =3.8, 3.9, 4.1, 4.2, 4.3, and 4.4 mm. The characteristic data of all these simulated resonance curves are listed in Table 1. Our simulation results

show that the resonance amplitude may exceed 20 dB when h is in a range from 3.9 mm to 4.3 mm, and that the resonance amplitude is less than 20 dB when h is 3.8 mm or 4.4 mm. The simulation results for h = 3.9, 4.0, 4.1, 4.2, and 4.3 mm are what we are interested in, for they are the typical resonance characteristics of our resonator matching the 50-Ω impedance. Using the simulated results of f_0 and Δf for h = 3.9, 4.0, 4.1, 4.2, and 4.3 mm, we calculated five Q values of our resonator matching the 50-Ω impedance. These Q values are also listed in Table 1.

Table 1. Simulated resonance characteristics of our resonator for different h values.

h/mm	f_0/MHz	resonance amplitude/dB	f_L/MHz	f_H/MHz	Δf/MHz	Q
3.8	466.254	18.1	465.894	466.608	0.714	
3.9	466.142	21.5	465.800	466.480	0.680	686
4.0	466.010	27.5	465.686	466.332	0.646	721
4.1	465.898	50.1	465.590	466.204	0.614	759
4.2	465.844	28.5	465.550	466.136	0.586	795
4.3	465.746	21.5	465.468	466.020	0.552	844
4.4	465.674	18.7	465.408	465.934	0.526	

The above simulation results are quite close to our practical measurement results. In our practical measurement, we used a screw arbor to continuously adjust the distance h between the resonator and the copper coil. We measured the values of resonant frequency f_0, 3-dB frequency band width Δf, and resonance amplitude of our resonator, when the values of h were 4.6, 4.7, 4.8, 4.9, 5.0, 5.1, and 5.2 mm. We can see that these measurement values listed in Table 2 are quite close to the simulated ones. Because the practically measured resonance amplitudes for h = 4.7, 4.8, 4.9, 5.0 and 5.1 mm were not less than 20 dB, we calculated Q values from the practically measured values of f_0 and Δf for these h values. These calculated Q values are also listed in Table 2.

Table 2. Practically measured resonance characteristics of our resonator for different h values.

h/mm	f_0/MHz	resonance amplitude/dB	Δf/MHz	Q
4.6	458.795	19.98	0.585	
4.7	458.773	24.30	0.559	821
4.8	458.758	30.57	0.533	861
4.9	458.743	32.63	0.510	899
5.0	458.728	25.85	0.495	927
5.1	458.698	21.96	0.488	940
5.2	458.683	18.66	0.458	

From the simulated and the practically measured resonance characteristics of our 50-Ω-impedance matched resonator, we can see that the resonant frequency f_0 of the 50-Ω impedance matched resonator decreases while the quality factor Q of the resonator increases as the distance h between the resonator and the copper coil increases. The dependences of the f_0 and the Q of the 50-Ω impedance matched resonator on distance h are shown in Fig. 3.

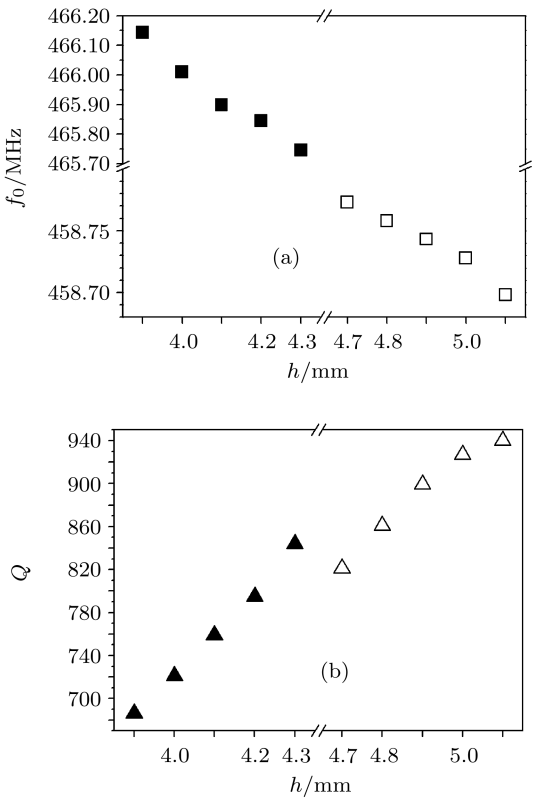


Fig. 3. Dependences of resonant frequency f_0 and quality factor Q of our 50-Ω impedance matched resonator on distance h between resonator and copper coil. Panel (a) shows that f_0 decreases as h increases. The solid squares represent the simulated f_0 values corresponding to different h values, while the open squares denote the practically measured ones. Panel (b) shows that Q increases as h increases. The solid triangles represent the simulated Q values corresponding to different h values, while the open triangles denote the practically measured ones.

Furthermore, comparing the simulated and practically measured resonant frequencies and quality factors of our resonator matching the 50-Ω impedance with the simulated eigenvalues of the resonant frequency and the quality factor of our resonator, we can see that the resonant frequency of our resonator matching the 50-Ω impedance is quite close to the eigenvalue of the resonant frequency of our resonator, but that the loaded quality factor of our resonator matching the 50-Ω impedance is very different from the eigenvalue of the unloaded quality factor of our resonator. We think it is natural that there is a large difference between the loaded and the unloaded quality factors of our resonator. However, the relationship between the loaded and the unloaded quality factors of our resonator seems to be not very simple, which needs to be further investigated in the future.

3. Conclusion

Using the ANSOFT HFSS, we simulated the resonant frequency and the quality factor of a dielectric resonator for the high-T_c rf SQUID when it is unloaded or matched a 50-Ω impedance. The simulated resonance characteristics of our dielectric resonator matching the 50-Ω impedance are quite close to the practically measured ones. The simulated and practically measured resonant frequencies of our resonator matching the 50-Ω impedance are all very similar to the simulated resonant frequency eigenvalue of our resonator without load, but the simulated and practically measured quality factors of our resonator matching the 50-Ω impedance are all quite different from the simulated unloaded quality factor eigenvalue of our resonator. Our study shows that the HFSS is quite suitable for simulating the dielectric resonator used for the high-T_c rf SQUID. We plan to carry out further studies on the characteristics of dielectric resonators for high-T_c rf SQUIDs by using the HFSS.

References

[1] Bednorz J G and Müller K A 1986 *Z. Phys.* B: *Condens. Matter* **64** 189

[2] Koelle D, Kleiner R, Ludwig F, Dantsker E and Clarke J 1999 *Rev. Mod. Phys.* **71** 631

[3] Daly K P, Dozier W D, Burch J F, Coons S B, Hu R, Platt C E and Simon R W 1991 *Appl. Phys. Lett.* **58** 543

[4] Zhang Y, Mück H M, Herrmann K, Schubert J, Zander W, Braginski A I and Heiden C 1992 *Appl. Phys. Lett.* **60** 645

[5] Zhang Y, Mück M, Braginski A I and Toepfer H 1994 *Supercond. Sci. Technol.* **7** 269

[6] Zhang Y, Zander W, Schubert J, Rüders F, Soltner H, Banzet M, Wolters N, Zeng X H and Braginski A I 1997 *Appl. Phys. Lett.* **71** 704

[7] Xie F X, Yang T, Ma P, Nie R J, Liu L Y, Wang F R, Wang S Z, Wang S G and Dai Y D CN1352469 [2002-06-05] (in Chinese)

[8] Zhang Y, Schubert J, Wolters N, Banzet M, Zander W and Krause H J 2002 *Physica* C **372–376** 282

[9] Liu X Y, Xie F X, Meng S C, Ma P, Yang T, Nie R J, Wang S Z, Wang F R and Dai Y D 2003 *Acta Phys. Sin.* **52** 2580 (in Chinese)

[10] Liu X Y, Xie F X, Meng S C, Dai Y D, Li Z Z, Ma P, Yang T, Nie R J and Wang F R 2004 *Chin. Phys.* **13** 100

[11] Mao H Y, Wang F R, Meng S C, Mao B, Li Z Z, Nie R J, Liu X Y and Dai Y D 2005 *Chin. J. Low Temp. Phys.* **27** 269 (in Chinese)

[12] He D F and Itozaki H 2006 *J. Appl. Phys.* **99** 123911